Polymer Dynamics in Dilute and Semidilute Solutions

Sanjay S. Patel* and Ken M. Takahashi

AT&T Bell Laboratories, 600 Mountain Avenue, Murray Hill, New Jersey 07974

Received November 11, 1991

ABSTRACT: Dielectric spectroscopy was used to probe the relaxation dynamics of dilute and semidilute polyisoprene solutions in a moderately good solvent. The concentration dependences of both the terminal relaxation time and the dielectric spectrum exhibit universality over a wide range of molecular weights. The terminal relaxation time in the limit of infinite dilution scales with $[\eta]M$ and is consistent with partially draining Rouse–Zimm behavior. Terminal times are exponential in concentration $\tau_1/\tau_1^0 = \exp(cA)$, where the concentration scaling parameter A has a somewhat different molecular weight dependence than intrinsic viscosity $[\eta]$. The terminal times show no transition in behavior with increasing concentration that would indicate the onset of entanglement. The spectrum of relaxation times appears to be a universal function of cA or $c[\eta]$. At low concentrations, $c[\eta] < 1$, the spectrum is consistent with Rouse–Zimm theory. At higher concentrations (up to $c[\eta] \approx 8$), loss peaks are much broader than the Rouse–Zimm prediction and, along with coil dimensions, become comparable to those seen in the melt for both entangled and unentangled polyisoprenes. Both the shape of the dielectric loss peaks and the dependence of characteristic concentration on molecular weight suggest that relaxation dynamics are controlled by the degree of overlap between polymer chains but not by intermolecular hydrodynamic interactions or by entanglements as they are usually defined.

Introduction

The viscoelastic behavior of polymers critically determines their processability and mechanical properties in many industrially important applications. Polymer properties stem from the configurations of their stringlike molecules, and the viscoelasticity of polymers is therefore quite different from that exhibited by metals and other materials composed of small molecules. It is important to achieve a fundamental understanding of how the size and shape of these long-chain molecules affect their motion because of the direct impact on the processing and end-use of these materials.

Polymers are often processed and used in the form of solutions. Polymer solutions are usually divided into three concentration regimes, namely, dilute, semidilute, and concentrated or melt regimes, based on the equilibrium dimensions of the molecules. One measure of molecular size is the root-mean-square end-to-end distance R, and for a polymer this quantity usually scales as

$$R = \langle \mathbf{R}^2 \rangle^{1/2} \sim M^{\nu} \tag{1}$$

where $\mathbf{R}$ is the end-to-end vector,[1] M is the molecular weight of the polymer, and ν is the excluded-volume exponent which ranges from 0.5 for a Θ solvent to $\approx$0.6 for a good solvent.[2] In the dilute regime, the polymer molecules are isolated and essentially noninteracting. As the concentration of the polymer is increased, intermolecular interactions become increasingly important. The onset of the semidilute regime is usually defined, although somewhat arbitrarily, as the concentration c^* where the solution concentration is equal to that within the volume occupied by an individual polymer molecule in the dilute regime. For a polymer in a good solvent, the transition from dilute to semidilute solutions is accompanied by a contraction in molecular size arising from the "screening" of the favorable monomer–solvent, or excluded-volume interactions. This contraction in chain dimensions with increasing concentration continues until the chains attain their Θ dimensions, demarcating the end of the semidilute regime and the onset of the concentrated solution regime. This transition concentration is usually denoted by c^{**}.

Besides the changes in molecular dimensions described above, the dynamics of the polymer chains are expected to change across the three concentration regimes due to differences in the degree of intermolecular interactions. In the dilute regime, intermolecular encounters are rare and the chain dynamics are known to be controlled by *intra*molecular hydrodynamic interactions, i.e., the effect the motion of one part of the molecule has on that of another by affecting the solvent flow field around it. As the concentration is increased, *inter*molecular hydrodynamic interactions become increasingly important and eventually the hydrodynamic interactions, like the excluded-volume interactions, are screened. This screening is intuitively expected since, by definition, there are no hydrodynamic interactions in polymer melts. At sufficiently high concentrations, the physical uncrossability of chain segments begins playing a dominant role leading to entanglement effects.

Although there seems to be a consensus on the underlying molecular models at the two extreme concentrations, namely, hydrodynamic interactions dominate at infinite dilution and entanglements dominate in polymer melts, the current understanding at intermediate concentrations is far from complete.[3] A variety of experimental techniques have been used to examine several aspects of polymer dynamics, and many of the heuristic arguments made above have been experimentally confirmed. The different aspects of polymer dynamics that are probed by various techniques are easily illustrated in terms of normal modes. In the framework of bead–spring models,[4] the motion of the polymer chain is that of a system of coupled oscillators. Normal-mode analysis decomposes the motion of the chain into coordinates each capable of independent motion.[5] The simplest case is that of the Rouse model where hydrodynamic interactions between the beads are neglected.[6] In this case, for a chain of N beads, the normal coordinates $\mathbf{X}_p$ are given by[5]

$$\mathbf{X}_p = \frac{1}{N}\int_0^N dn \cos\left(\frac{p\pi n}{N}\right)\mathbf{R}_n(t) \qquad p = 0, 1, 2, \ldots \tag{2}$$

where $\mathbf{R}_n$ represents the position of the nth bead. The inverse transform of the above equation is given by

$$\mathbf{R}_n = X_0 + 2\sum_{p=1}^{N}\mathbf{X}_p \cos\left(\frac{p\pi n}{N}\right) \tag{3}$$

As mentioned earlier, a variety of experimental techniques

0024-9297/92/2225-4382$03.00/0

are used to study polymer dynamics, and among these viscoelastic (zero-shear viscosity and dynamic moduli) measurements are the most common.[3] Polymer dynamics have also been proved by measurements of diffusion coefficients[7] and the birefringence of solutions subjected to oscillatory flow or electric fields.[8,9] Ignoring issues such as experimental sensitivity, the various techniques can be classified based on the particular aspect of the dynamics they measure.[10] In this scheme, viscoelastic and birefringence measurements belong to the same class since both the stress and the (intrinsic) birefringence are proportional to the anisotropy of chain orientations.[5] The stress σ can be expressed as

$$\sigma_{\alpha\beta} \sim \sum \left\langle \frac{\partial R_{n\alpha}}{\partial n} \frac{\partial R_{n\beta}}{\partial n} \right\rangle \sim \sum A_p \langle X_{p\alpha}(t)\, X_{p\beta}(t) \rangle \quad (4)$$

where A_p can be evaluated from eq 2 and 3 for the normal coordinates. Except for premultiplying constants, the expression for the intrinsic birefringence is exactly the same as that for the stress given above.

Diffusion measurements constitute a different class of techniques since they measure the displacement of the center of mass. The position of the center of mass $\mathbf{R}_{cm} = \mathbf{X}_0$ using the definition of the normal coordinates in eq 2. The diffusion coefficient D is defined by the mean-square displacement of the center of mass and can therefore be expressed as

$$D \sim \frac{\langle (\mathbf{R}_{cm}(t) - \mathbf{R}_{cm}(0))^2 \rangle}{t} \sim \frac{\langle (\mathbf{X}_0(t) - \mathbf{X}_0(0))^2 \rangle}{t} \quad (5)$$

Another technique that can be used to probe polymer dynamics is dielectric relaxation spectroscopy.[11] This technique measures the complex permittivity $\epsilon^*(\omega) = \epsilon' - i\epsilon''$ of a system ($i^2 = -1$) over a wide range of frequency ω. Of particular interest, in the context of studying long-chain dynamics, is the case of polymers with a persistent component of dipole moment along the chain backbone (type-A chains in Stockmayer's notation[11]), where $\epsilon^*(\omega)$ can be related to the correlations in the end-to-end vector of a polymer chain.[11-13] The end-to-end vector can be expressed in terms of normal coordinates, $\mathbf{R}(t) \equiv \mathbf{R}_N(t) - \mathbf{R}_0(t) = -4\sum_{p=\text{odd}} \mathbf{X}_p(t)$, and the correlation in the end-to-end vector can therefore by expressed as $\langle \mathbf{R}(t)\cdot\mathbf{R}(0) \rangle = 16\sum_{p=\text{odd}} \langle \mathbf{X}_p(t)\cdot\mathbf{X}_p(0) \rangle$. For type-A polymers, $\epsilon^*(\omega)$ is related to this correlation by

$$\epsilon^*(\omega) - \epsilon_\infty = \Delta\epsilon \int_0^\infty -\frac{d}{dt}\left(\frac{\langle \mathbf{R}(t)\cdot\mathbf{R}(0) \rangle}{\langle \mathbf{R}^2 \rangle} \right) e^{(-i\omega t)}\, dt \quad (6)$$

where ϵ_∞ is the unrelaxed dielectric constant and $\Delta\epsilon$ is the strength of the relaxation. A comparison of eq 4–6 clearly shows that the three classes of techniques described above are very different probes of the polymer dynamics. In other words, these techniques measure different aspects of the dynamics and are perhaps best viewed as being complementary.

To improve our understanding of the dynamics of long-chain polymers, it is important to examine several different measures of the dynamics. To date, systematic studies of polymer dynamics in dilute and semidilute solutions have predominantly been done using techniques in the viscoelastic and diffusion categories described above.[9,14] Dielectric measurements of polymer relaxation have been made by Adachi and Kotaka,[15] mostly on melts and concentrated solutions. They have shown the *cis*-polyisoprene (PI) is a Stockmayer type-A molecule; that is, it possesses a net axial dipole moment. PI has the advantages that it can be made anionically with narrow molecular weight distributions and that it is compatible with nonpolar solvents.

Table I
Molecular Characteristics

polymer	M_w[a]	M_w/M_n[b]	$[\eta]$[c]
31K	30.7	1.03	28.1
63K	63.4[d]	1.02	44.6
115K	115.1	1.02	
132K	131.7	1.04	75.2
305K	305.5	1.04	126.6
306K	306.4	1.04	
454K	454.3	1.06	173.0
1.3M	1260.0	1.03	360.0
3.3M	3270.0	1.04	745.8

[a] Weight-average molecular weights of polyisoprenes, in thousands, determined by the manufacturer using light scattering. [b] Determined using size-exclusion chromatography by the manufacturer. [c] Intrinsic viscosity in cm^3/g. [d] Determined by the manufacturer using size-exclusion chromatography (light scattering molecular weight not measured).

These properties make PI an ideal subject for dielectric studies of polymer dynamics, a fact that the Kotaka group,[15-19] and recently Boese, Kremer, and co-workers,[20] have used to great advantage. Our measurements were also done on PI solutions with the same advantages in mind. We present here the first systematic dielectric study in the dilute and semidilute concentration regimes. We compare our results to these obtained by other techniques and discuss our findings in the context of the current theoretical understanding of polymer solutions.

Experimental Section

Materials. Linear polyisoprene samples with narrow molecular weight distributions were obtained from Polymer Laboratories (Church Stretton, U.K.) and used in this study without further purification. The molecular characteristics of these samples provided by the manufacturer are listed in Table I. The microstructure of these polymers was determined by the manufacturer using proton NMR as being predominantly cis (87% cis, 9% trans, and 4% vinyl). The solvent used in this study was Isopar-G. It was obtained from Exxon Chemicals and was used as received. Isopar-G is a hydrocarbon solvent consisting of branched alkanes, predominantly dimethyloctane. This solvent has a dielectric constant of 2.000 in the experimental frequency range (160 Hz to 1 MHz) and was selected for its very high dielectric purity. All solutions were prepared by weight. The density of the solvent ρ_s was measured to be 0.742 g cm^{-3} at 25 °C. Using this value along with the polymer density $\rho_p = 0.913$ g cm^{-3},[22] concentrations were converted to g cm^{-3} assuming volume additivity. The solutions were prepared by direct addition of solvent to polymer, and solvation was assisted by occasional gentle shaking over 2–7 days. The solutions were filtered through 1-μm PTFE filters (Gelman) prior to use.

Viscosity Measurements. Kinematic viscosity measurements were made using Ubbelohde tubes immersed in a constant-temperature bath on a Schott-Geräte AVS 310 viscometer. All the measurements were made in either one of two tubes, one with a capillary diameter 0.46 mm and the other 0.53 mm, both of length 9.2 cm. The temperature of the bath was maintained at 25 ± 0.01 °C. The kinematic viscosity of the solvent was measured to be 1.404 cS using the 0.53-mm tube calibrated with deionized water at 25 °C. Using this value along with the measured ρ_s, the viscosity of solvent $\eta_s = 1.042$ cP.

Dielectric Measurements. Dielectric measurements were made in a circular parallel-plate molybdenum cell having a radius of 5.08 cm and an electrode separation of 100 μm. The complex permittivity $\epsilon^*(\omega)$ was measured with a Hewlett-Packard 4284A automated bridge over a frequency range of 160 Hz to 1 MHz. The measurements were made at 25 ± 1 °C. Calibration to correct for stray admittances and instrument error along with extensive data averaging reduced the uncertainty in $\tan\delta = \epsilon''/\epsilon'$ to an estimated 6×10^{-6} over the frequency range 300 Hz to 400 kHz and 2×10^{-5} in the ranges 160–300 Hz and 400 kHz to 1 MHz. For all except the highest molecular weight samples, dielectric loss data whose errors were greater than 5% of the peak height were not used. Because the loss peaks for the highest molecular

weight samples resided in the relatively noisy low-frequency regime, data whose errors were up to 10% of the peak height were used.

Results and Discussion

Dilute-Solution Viscosities. It has been well established that the (zero-shear rate) viscosity η of a dilute polymer solution can be expressed as[21]

$$\eta = \eta_s(1 + (c[\eta]) + k_H(c[\eta])^2 + ...) \quad (7)$$

where c is the polymer concentration in mass per unit volume. The constants $[\eta]$, the intrinsic viscosity of the polymer, and k_H, the Huggins coefficient, characterize the particular polymer–solvent system under consideration. It will be useful to relate viscosity and dielectric relaxation data by making the analogy to a suspension of hard spheres. The Einstein expression, analogous to eq 7, for the viscosity of a dilute suspension is

$$\eta = \eta_s(1 + 2.5\phi + 4\phi^2 + ...) \quad (8)$$

where ϕ is the volume fraction of hard spheres. For a dilute polymer solution, assuming volume additivity

$$\phi \approx \frac{cN_A}{M}\frac{4}{3}\pi R_g^3 \quad (9)$$

where N_A is Avogadro's number. A comparison of eq 7–9 shows that $[\eta]$ is expected to be proportional to the volume of a polymer molecule which clearly depends on the molecular weight of the polymer and the thermodynamic quality of the solvent as expressed in eq 1. Of course, solvent molecules penetrate the polymer coil, so the hydrodynamic, or effective, hard-sphere radius R_h is different from R_g. The intrinsic viscosity is usually expressed as[2]

$$[\eta] = \Phi\frac{R^3}{M} = KM^a \quad (10)$$

where the differences arising from the use of different measures of size, namely, R, R_g, and R_h, are lumped along with other constants in the Flory–Fox constant Φ. Alternatively, the intrinsic viscosity is expressed in terms of a power law, the Mark–Houwink–Sakurada (MHS) equation, where K and a ($=3\nu - 1$) are the corresponding polymer- and solvent-dependent parameters. For a polymer in a good solvent, for example, PI in cyclohexane at 25 °C, $a \approx 0.75$.[23]

Viscosity measurements were made for 7 PI molecular weights at 12 concentrations of each polymer in Isopar-G. The intrinsic viscosity $[\eta]$ and the Huggins coefficients k_H were determined by plotting both the specific viscosity $\eta_{sp} = (\eta - \eta_s)/\eta_s$ (Huggins plot) and the inherent viscosity $\eta_{inh} = \ln(\eta/\eta_s)/c$ (Mead–Fuoss plot) as functions of concentration. Both these plots are linear for low concentrations, and the common intercept of both these plots is $[\eta]$. The extrapolations were done over a concentration range for which $c \ll 1/[\eta]$ to ensure linearity of both the plots. The slopes of these plots are related to the Huggins coefficient ($=k_H$ for the Huggins plot and $=k_H - 1/2$ for the Mead–Fuoss plot). The Huggins coefficient k_H was found to be 0.42 over the entire molecular weight range examined and lies within the range 0.4–0.6 reported for several other polymers in marginal solvents.[22] The values of $[\eta]$ obtained from the intercepts are listed in Table I.

A double-logarithmic plot of $[\eta]$ as a function of M_w is shown in Figure 1. The MHS equation fits the data well with

$$[\eta] = 1.94 \times 10^{-2} M_w^{0.70} \text{ cm}^3/\text{g} \quad (11)$$

The value of $a = 0.70$ indicates that the solvent is marginal

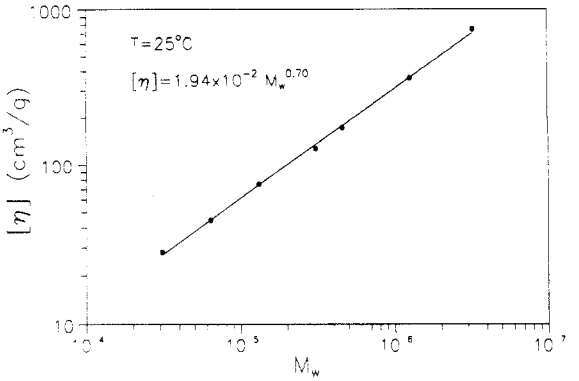

Figure 1. Intrinsic viscosity as a function of molecular weight.

compared to cyclohexane and toluene.[23] On the basis of this data, $\nu = 0.567$ for PI in Isopar-G, again indicative of a marginal solvent.

When a solution is subjected to high shear rates, the polymer molecules are stretched far from their equilibrium configurations and the intrinsic viscosity exhibits shear thinning.[24,25] Although these shear-thinning effects are interesting, in this study we want to focus on the dynamics of polymers in their equilibrium configurations, and it is important to gauge the importance of these shear-thinning effects in our viscosity measurements. Noda et al.[24] have empirically shown that for high molecular weight polymers the onset of shear thinning occurs at a dimensionless shear rate characterized by a Deborah number $De = \dot{\gamma}\lambda$ on the order of 1.0, where $\dot{\gamma}$ is the shear rate and λ is a characteristic (longest) relaxation time for the polymer.[26] The maximum shear rates in this study were approximately 1200 s^{-1} based on the capillary dimensions. To estimate the molecular relaxation time, we return to the hard-sphere model. The rotational time for a hard sphere is related to its volume V by

$$\lambda = 3\eta V/k_B T \quad (12)$$

where k_B is the Boltzmann constant and T the absolute temperature.[27] For dilute solutions $\eta = \eta_s$, and this relaxation time can be expressed in terms of the hard-sphere intrinsic viscosity as

$$\lambda = \frac{[\eta]\eta_s M}{0.833 N_A k_B T} \quad (13)$$

using eqs 7–9. Strictly speaking, the MHS exponent (eq 10) is 1 for the Rouse model and 0.5 for the Zimm model, neither of which treats excluded-volume effects in moderate or good solvents. By analogy to the hard-sphere model (eqs 8–10), however, the use of measured (eq 11) rather than predicted intrinsic viscosities to calculate λ approximately accounts for molecular volume effects in the context of Rouse–Zimm theory. It is important to note that the hard-sphere relaxation time then is on the order of the longest relaxatin time τ_1 predicted by Rouse–Zimm theories and differs from these only by a constant factor. (For viscoelastic measurements, the constant 0.833 in the above equation is replaced by 1.645 for the Rouse model and 2.369 in the Zimm model with dominant hydrodynamic interaction.[25,28] Furthermore, τ_1(dielectric) $= 2\tau_1$(viscoelastic) due to inherent differences in the quantities being measured as discussed earlier.[28]) As mentioned earlier, it is well established that the Zimm model describes polymer relaxation at infinite dilution reasonably well. Using the empirically determined MHS

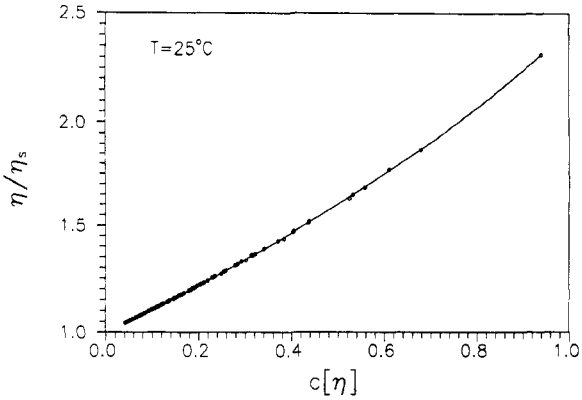

Figure 2. Viscosity as a function of $c[\eta]$.

parameters in eq 11 along with the values of other fundamental constants at 25 °C

$$\lambda = 3.443 \times 10^{-15} M^{1.7} \text{ s} \quad (14)$$

based on the Zimm model for dominant hydrodynamic interactions. The upper bound on the Deborah number for the viscosity measurements reported here is 0.49, so we conclude that the molecules are not distorted far from their equilibrium shapes.

The viscosity for all seven molecular weights is plotted as a function of $c[\eta]$ in Figure 2. The data collapse onto a universal curve as expected from eq 7. This behavior is not unique to our data and is a well-established result in the polymer literature.[21] Since eq 7 is a power series in $c[\eta]$, one might expect a finite representation of this series to fit the data only for $c[\eta] \ll 1$. However, Figure 2 clearly shows that the dilute-solution description of the viscosity of these polymer solutions, namely, eq 7 with $k_H = 0.42$, continues to fit the data even at concentrations where $c[\eta] \approx 1$. Deviations from the dilute-solution behavior are expected when the system crosses over into the semidilute regime where there is significant overlap between individual polymer molecules. Because the intrinsic viscosity is proportional to the volume of the polymer molecule in solution, the product $c[\eta]$ is a measure of the degree of overlap between polymer coils analogous to c/c^*, and deviations from dilute-solution behavior are expected to become increasingly significant beyond some value $(c[\eta])^*$. Based on the viscosity data in Figure 2, $(c[\eta])^* > 0.94$.

Dielectric Relaxation. The complex permittivity $\epsilon^*(\omega)$ was measured for five polymers with molecular weights ranging from about 30 000 to 1 200 000 at a series of concentrations. The data for the dielectric loss ϵ'' are plotted in Figure 3a–e. One measure of the characteristic relaxation time is the peak frequency; that is, $\lambda \sim \omega_{peak}^{-1}$. A direct comparison of the loss data in Figure 3 shows that the peaks in the dielectric loss for the higher molecular weight polymers have a longer characteristic relaxation time as intuitively expected. Furthermore, for any given molecular weight, the peak position shifts to lower frequencies with increasing concentration, indicating a slowing down of the molecular relaxation. To examine the effects of molecular weight and concentration on relaxation dynamics more quantitatively, we used an optimization procedure (described below) to obtain the characteristic amplitude and frequency of the molecular relaxation from the dielectric loss data.

In dielectric relaxation spectroscopy the loss factor ϵ'' contains a nonzero component when the applied frequency is comparable to molecular relaxation frequencies. Rigid polar molecules that relax with only a single characteristic

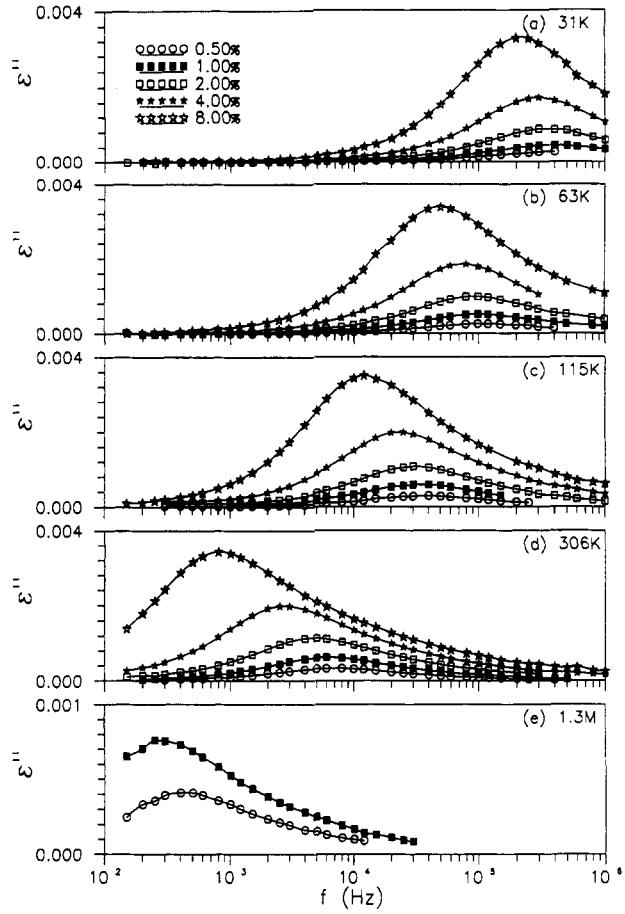

Figure 3. Concentration and molecular weight dependence of the dielectric loss as a function of frequency.

time exhibit dielectric loss peaks of the Debye form[11]

$$\epsilon''(\omega) = \Delta\epsilon \frac{\omega\tau_1}{1 + \omega^2\tau_1^2} \quad (15)$$

However, when a system can relax over a wide range of time scales, as in the case of flexible polymers, the contributions to the loss peak are additive and ϵ'' can be expressed as

$$\epsilon''(\omega) = \Delta\epsilon \int_{-\infty}^{\infty} g(\tau) \frac{\omega\tau}{1 + \omega^2\tau^2} \, d \ln \tau \quad (16)$$

The molecular relaxation dynamics are completely characterized by the spectrum $g(\tau)$ which represents the intensity of the relaxation mode with time constant τ.[29]

It has been observed that the low-frequency portion of the loss peak takes the form of a single relaxation; that is, it obeys eq 15 with $\epsilon''_{max} = \Delta\epsilon/2$. This region is analogous to the terminal zone of the loss modulus $G''(\omega)$ observed in dynamic mechanical measurements and represents the longest relaxation time constant τ_1 for molecular relaxation.[3] To characterize this terminal relaxation, the terminal time τ_1 and the peak height ϵ''_{max} were determined by a least-squares procedure that minimized the sum of squares of the difference between the loss data on the low-frequency side of the loss peak $0.1 < \epsilon''/\epsilon''_{max} < 1$ and the right-hand side of eq 15.

Parameters obtained using such a fitting procedure are comparable to those obtained by simply picking out the amplitude ($=\epsilon''_{max}$) and frequency ($\tau_1 = 1/\omega_{max}$) of the loss maximum. The fitting procedure has the advantage of noise averaging and allows the peak position to be determined more precisely. However, although the shape of the low-frequency tail of the loss peak has the form of

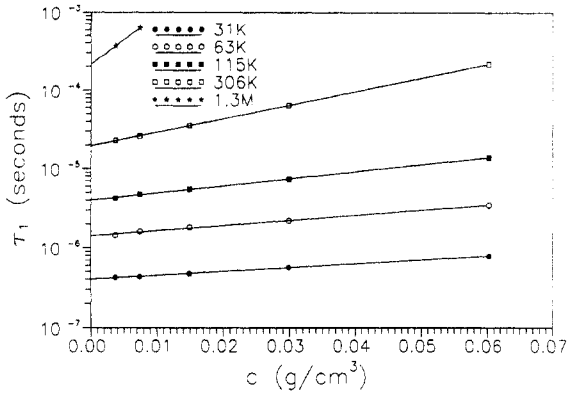

Figure 4. Concentration dependence of the terminal relaxation time.

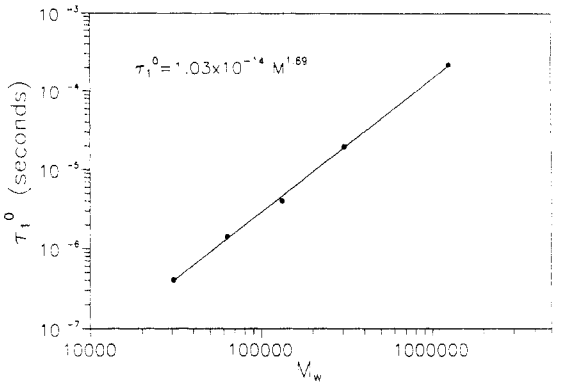

Figure 5. Terminal relaxation time at infinite dilution.

a single relaxation, it contains finite contributions from higher-frequency relaxations as well as the terminal relaxation. As a result, the height and frequency of the loss maximum will depend to some extent on the entire spectrum $g(\tau)$. For example, for a system following Rouse dynamics, the dielectric loss

$$\epsilon''(\omega) = \frac{8\Delta\epsilon}{\pi^2}\sum_{p=\text{odd}}\frac{1}{p^2}\frac{\omega\tau_p}{1+\omega^2\tau_p^2}, \quad \tau_p = \tau_1/p^2 \qquad (17)$$

has a peak position (ω_{max}) and a peak height (ϵ''_{max}) that are 3% higher than those based on the terminal relaxation ($p = 1$) alone. Note that the contribution of high-p modes is deemphasized in dielectric measurements by the $1/p^2$ weighting; loss data are primarily sensitive to the longest relaxation times. Applying the fitting procedure described above to the Rouse spectrum, the calculated terminal relaxation time is between τ_1 and $1/\omega_{max}$; the best-fit relaxation time is 1.5% smaller than τ_1. We conclude that the fitted relaxation times and peak heights are close to the true terminal values but caution that they contain a small spectrum-dependent contribution. Further, it should be noted that the peak height ϵ''_{max} is primarily indicative of the terminal relaxation, while the strength of the relaxation $\Delta\epsilon$ is proportional to the area under the loss peak ϵ'' (ln ω). Therefore, the estimated ϵ''_{max} will be less than $\Delta\epsilon/2$. For the Rouse spectrum, this error will be a factor of $\pi^2/8$.

The longest relaxation times τ_1, extracted from the data in the manner described above, are plotted in Figure 4 as a function of concentration for the various molecular weights. The longest relaxation time shows a smooth, monotonic increase with increasing concentration for all the molecular weights. Although no concentration-independent regime is discernible at low concentrations from Figure 4, we note that the data are fit reasonably well by an exponential function. Such fits allow us to extract relaxation times at infinite dilution by extrapolation to zero concentration. These infinite-dilution relaxation times, τ_1^0, are plotted in Figure 5 as a function of molecular weight and can be fit reasonably well using

$$\tau_1^0 = 1.03\times10^{-14}M^{1.69}\ \text{s} \qquad (18)$$

The molecular weight exponent, namely, 1.69, is reasonably close to the value of 1.7 predicted by the hard-sphere model based on intrinsic viscosity data ($\tau_1^0 \sim M^{3\nu} \sim M^{1.7}$) and lies between the values of 1.5 and 2 predicted by the Zimm and Rouse models, respectively. Therefore, our system can perhaps be characterized as partially-draining.

As discussed earlier in the context of eq 13, the longest relaxation time for the Rouse, Zimm, and hard-sphere models can be calculated *without any adjustable parameters* using the measured values of the intrinsic viscosity.

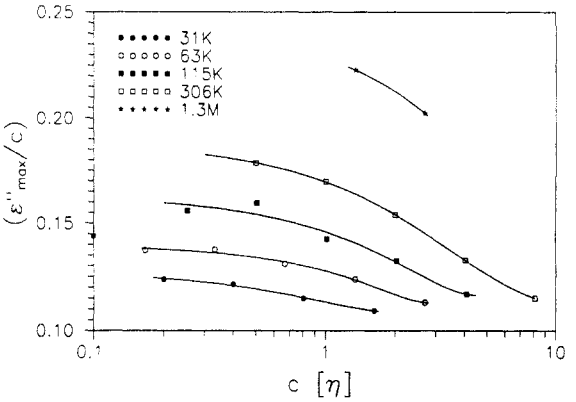

Figure 6. Concentration dependence of the height of the dielectric loss peak, showing collapse of coil dimensions $\langle R^2\rangle/M \sim \Delta\epsilon/c$ with increasing volume fraction $c[\eta]$.

For the Rouse model, the ratio of the observed and predicted longest relaxation times varies in the range 0.9–0.94. (The variation is due to the small mismatch in the molecular weight dependence of the observed and predicted relaxation times, namely, $M^{1.69}$ and $M^{1.7}$, respectively.) The corresponding range for the Zimm model is 1.3–1.35. This comparison again suggests that our system is best described as partially draining and that the Rouse–Zimm and hard-sphere models are reasonably quantitative for the longest relaxation time using measured intrinsic viscosities.

The strength of the dielectric relaxation for type-A polymers is related to the mean-square end-to-end distance by

$$\frac{\Delta\epsilon}{c} = \left(\frac{4\pi N_A\mu^2F}{3k_BT}\right)\left(\frac{\langle R^2\rangle}{M}\right) \qquad (19)$$

where μ is the dipole moment per unit contour length and F the ratio of the internal and external electric fields.[11] Therefore, $\Delta\epsilon$ is a measure of the coil size in solution. At low concentrations, we expect the polymer coils to be swollen and $\langle R^2\rangle/M \sim M^{2\nu-1} \sim M^{0.13}$. At high concentrations, the excluded-volume interactions are expected to be screened and $\langle R^2\rangle/M \sim M^0$. As noted above in the description of the fitting procedure used to extract the terminal relaxation behavior, ϵ''_{max} is proportional to $\Delta\epsilon$ but the proportionality constant is spectrum dependent. Despite this complication, it is instructive to plot (ϵ''_{max}/c) as a function of the degree of overlap between molecules $c[\eta]$ for the various molecular weights as shown in Figure 6. This plot shows that the data are consistent with eq 19; the higher molecular weight samples are more swollen than the lower molecular weight polymers due to the excluded-volume interactions and therefore exhibit greater shrinkage when these interactions are screened. Furthermore, there is a noticeable similarity in the observed

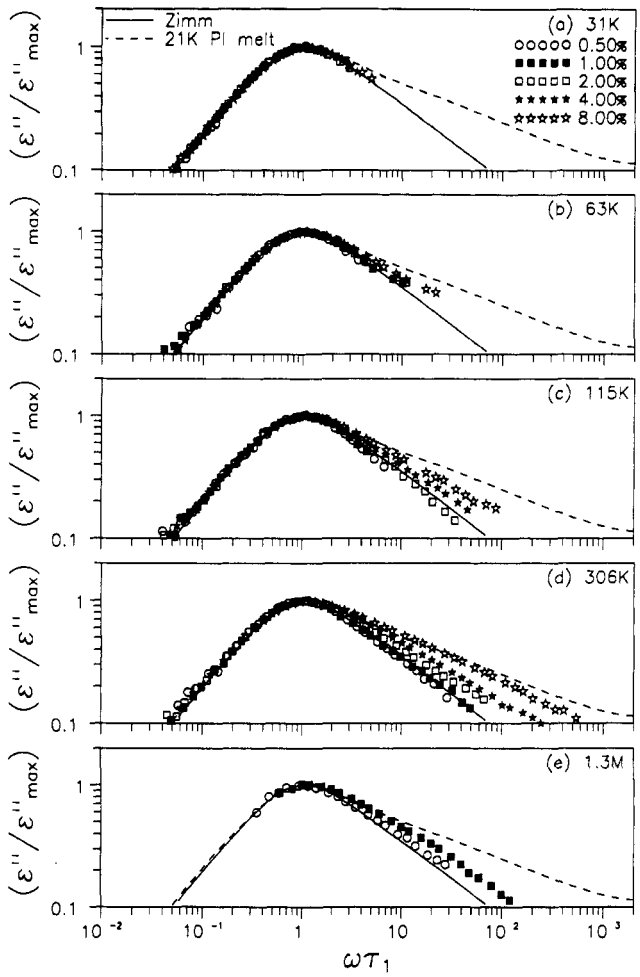

Figure 7. Concentration and molecular weight dependence of normalized loss peaks. The loss peaks appear to broaden from the Rouse–Zimm prediction (solid line) at low concentration, approaching the melt behavior of Imanishi et al.[17] (dashed line) at higher concentrations.

concentration dependence of the coil size for the various molecular weights suggestive of a universality in the crossover from dilute to semidilute solutions. Although we expect the trends to be qualitatively correct, we do not quantify the coil contraction in light of the fact that ϵ''_{max} is only a approximate measure of $\Delta\epsilon$ as discussed earlier. However, these data do suggest that there is appreciable shrinkage in the coil size across the concentration range over which the dielectric measurements were made.

The longest relaxation time essentially determines the *location* of the dielectric loss peak. However, the *shape* of the peak is determined by the spectrum of relaxation times $g(\tau)$. To examine the effect of concentration on the relaxations faster than the terminal time, the measured dielectric loss peaks are normalized using the values of τ_1 and ϵ''_{max} discussed earlier, and the resultant curves are plotted in Figure 7a–e. For all five molecular weights the dielectric loss curves at various concentrations collapse onto a single curve for $\omega\tau_1 < 1$ as a result of this normalization, and this collapsed curve is indistinguishable from a Debye relaxation centered at $\omega\tau_1 = 1$. These plots, especially the ones for the higher molecular weights, clearly show that the normalized loss curves broaden with increasing concentration. Therefore, the concentration affects both the longest relaxation time (peak position) and the relaxation spectrum (shape of peak).

As discussed earlier, the Zimm model with dominant hydrodynamic interactions is reasonably quantitative in describing the longest relaxation times for our system in the limit of infinite dilution. Figure 7 shows that this model also works reasonably well in predicting the shape of the dielectric loss peak at low concentrations for all five molecular weights. It is important to note that the Zimm ($\tau_p \approx \tau_1/p^{3/2}$) and Rouse ($\tau_p \approx \tau_1/p^2$) models are essentially indistinguishable over the range of dielectric loss shown in Figure 7. The data for a 21 000 molecular weight PI melt reported by Imanishi et al.[17] are also plotted in Figure 7, and a comparison with this data suggests that the spectrum continuously evolves from being Rouse–Zimm-like at low concentration to being meltlike at high concentrations.

Dynamic Scaling Based on the Degree of Overlap between Molecules. In an effort to establish a suitable framework for quantifying the observed effects of concentration on the dynamics of polymer chains, we briefly discuss the effects *expected* heuristically. For this purpose, a natural starting point is the well-established infinite-dilution regime where the dynamics of isolated molecules are dominated by the intramolecular hydrodynamic interactions. The nondraining Zimm and hard-sphere models are reasonably quantitative in this regime as discussed earlier in the context of the longest relaxation time τ_1^0. As shown in Figure 7, the relaxation spectrum based on the Zimm model also predicts the shape of the dielectric loss peak reasonably well in this regime. Therefore, to a very good approximation, isolated polymer molecules are essentially nondraining and bear a strong resemblence to hard-sphere suspensions at infinite dilution.

At finite but low concentrations, the dynamics are complicated by intermolecular interactions and the understanding is far less established. One possible scenario is that the molecules may retain some of their infinite-dilution hard-sphere characteristics and increasing the concentration leads to intermolecular hydrodynamic interactions, again akin to hard-sphere suspensions. Here, the interaction is expected to depend on the volume occupied by the individual molecules, or alternatively, by analogy to hard spheres, on the volume fraction ϕ of polymer in solution. As discussed earlier, since the intrinsic viscosity $[\eta]$ is proportional to the hydrodynamic volume of a polymer coil, the volume fraction can be expressed in terms of $c[\eta]$. Therefore, as pointed out by Frisch and Simha,[21,30] if the change in coil dimensions with increasing concentration due to screening of excluded-volume interactions is neglected, $c[\eta]$ is a measure of the degree of overlap between polymer molecules in solution. Even if the reduction in coil size is itself a function of the degree of overlap between polymer coils as suggested by the data in Figure 6, $c[\eta]$ can be expected to remain as the appropriate concentration variable. Therefore, in this scenario, the dynamics of polymer coils in dilute and semidilute solutions are expected to be a universal function of $c[\eta] \sim cM^a$ where a is the MHS parameter (=0.7 for our system).

It is important to note that the product $c[\eta]$ is analogous to the ratio c/c^* where the overlap concentration c^*, like the intrinsic viscosity, is also usually based on the infinite dilution dimensions of the polymer molecule. In support of the heuristic arguments made above, it must be noted that several static quantities like the osmotic pressure and the radius of gyration of a polymer coil have been shown to be universal functions of c/c^*.[31,32] Furthermore, dynamic quantities like the zero-shear viscosity data shown in Figure 2 also show universality with $c[\eta]$. In fact, studies on several polymer–solvent systems have demonstrated that the viscosity data for each system at different concentrations and molecular weights can be reduced reasonably well to a single master curve in terms of $c[\eta]$.[21] This universal function of $c[\eta]$ has been observed up to concentrations as high as 50%.[33,34] Therefore, the uni-

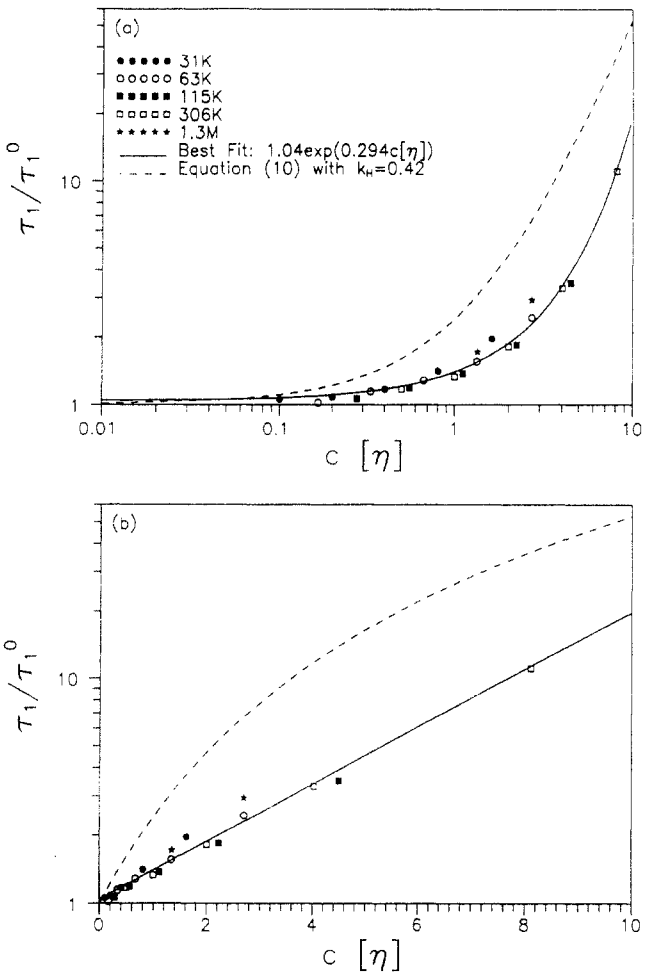

Figure 8. Reduced terminal relaxation time as a function of dimensionless concentration $c[\eta]$. The solid line is the best-fit exponential, while the dashed line shows the concentration dependence of the solution viscosity. a and b are log–log and semilog representations of the data for the five molecular weights.

versality of polymer static and dynamic properties in terms of $c[\eta]$ in dilute and semidilute solutions seems fairly well established. However, it has also been reported that the collapse of the viscosity data onto a master curve can be improved if the data are reduced using $cM^{a'}$, instead of cM^{a}.[33,34] In these cases, the empirically chosen values of a' are quite close, but not equal to, the MHS parameter a obtained from intrinsic viscosity measurements. In other words, the viscosity is, strictly speaking, only an approximate function of $c[\eta]$.

We now examine our dielectric data for this apparent universality in terms of $c[\eta]$. In fact, the data for the concentration dependence of the longest relaxation time for all the molecular weights examined in this study collapse reasonably well onto a universal curve as shown in Figure 8. However, the collapse is not perfect, and, as we will show later, the data can be better reduced to a master curve using a different strategy. In other words, the longest relaxation time is approximately a universal function of $c[\eta]$ over the entire concentration range of our measurements, namely, $0.1 < c[\eta] < 8.15$.

It is interesting to compare the observed concentration dependence of the longest relaxation time with that expected from a simple hard-sphere model expressed in eqs 12 and 13. In the hard-sphere model, one simple scenario is where increasing the concentration simply increases the viscosity of the medium, thereby slowing down the relaxation of the molecule. Therefore, the concentration dependence of the relaxation time is exactly that of the viscosity, and for the sake of comparison, our

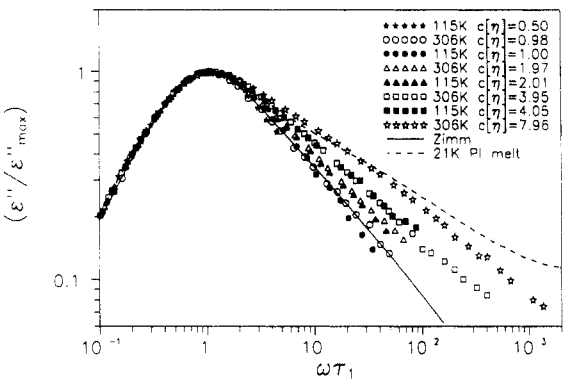

Figure 9. Normalized dielectric loss peaks for 115K (solid symbols) and 306K (open symbols) PI samples. For common values of $c[\eta]$ (1.0 (circles), 2.0 (triangles), and 4.0 (squares)), the loss peaks appear to be identical. At low concentrations $c[\eta] < \approx 1$, the shape of the loss peak is close to the Zimm prediction. At the highest concentration ($c[\eta] \approx 8$), the loss spectrum approaches that of the melt.[17]

measured concentration dependence of the viscosity, namely, eq 7 with $k_H = 0.42$, is also plotted in Figure 8. Clearly, this model is too simplistic and predicts a stronger concentration dependence than is actually observed in the low concentration region $c[\eta] < 3$. According to eq 12, the weak concentration dependence of τ_1 suggests that the molecules do not sense the effective viscosity of the medium, since we know that coil size is not sensitive to concentration when $c[\eta] \ll 1$ (Figure 6).

As discussed above, the data in Figure 8 show that the longest relaxation time is approximately a universal function of the degree of overlap between polymer molecules. Furthermore, a direct comparison of some of the normalized peaks shown in Figure 9 indicates that the relaxation spectrum also seem to be a universal function of $c[\eta]$. This comparison shows that the broadening of the relaxation spectrum with increasing polymer concentration, noted earlier in Figure 7, is simply a function of the degree of overlap between polymer molecules and evolves from being Rouse–Zimm-like at low concentrations to being meltlike at high concentrations. Therefore, both our viscosity and dielectric measurements show that the dynamics of polymer solutions are approximately a function of $c[\eta]$ only, at least over the dilute and semidilute concentration range examined in this study.

Effects of Entanglements. Longest Relaxation Time. As seen in Figures 8 and 9, our data extend up to $c[\eta] \approx 8$ where one would expect significant overlap between polymer coils which in turn should promote entanglements. In an effort to elucidate the observed universal concentration dependence, it is useful to assess the effect of entanglements on our measurements. Imanishi et al.[17] have empirically shown that, for PI melts, the onset of entanglements dramatically increases the molecular weight dependence f the longest relaxation time ($\tau_1 \sim M^2$ for unentangled polymers and $\tau_1 \sim M^{4\pm0.2}$ for entangled polymers). The same effect has been demonstrated by Adachi and co-workers[18] for concentrated PI solutions in toluene. Osaki et al.[35] report that their empirically determined entanglement molecular weight M_e for polystyrene solutions in Aroclor can be fit using the following equations:

$$cM_e = 2 \times 10^4 \quad c \geq 0.3 \text{ g cm}^{-3}$$

$$c^{1.4}M_e = 1.23 \times 10^4 \quad c < 0.3 \text{ g cm}^{-3} \qquad (20)$$

All our measurements were done at $c < 0.3$ g cm^{-3}, and in

order to apply this entanglement criterion to our system, we interpret it as

$$c^{1.4}M_e = 0.3^{0.4}\rho_p M_e^0 \qquad c < 0.3 \text{ g cm}^{-3} \tag{21}$$

where M_e^0 is the entanglement molecular weight in the melt state. In fact, since for our system $[\eta] \sim M^{0.7} \approx M^{1/1.4}$, the above criterion for the concentration at which the solution is entangled can be expressed in terms of a criterion in $c[\eta]$. Ignoring chemical differences between the two systems and assuming that the quality of the solvent is the same in both cases, PI solutions in Isopar-G are expected to be entangled at $c[\eta] \approx 5.8$ based on the above criterion using the known value of ρ_p and the literature value of $M_e^0 = 5000$ for PI melts.[36] Figure 8a shows that, at the highest concentration ($c[\eta] \approx 8$), τ_1 indeed increases with concentration faster than the extrapolated dilute-solution viscosity (dashed line). However, although the collapse onto a master curve is not perfect, the data over the entire concentration range is fit reasonably well by

$$(\tau_1/\tau_1^0) = 1.04e^{0.294c[\eta]} \tag{22}$$

as shown in Figure 8b. Therefore, our data support the heuristic view that entanglements do not set in any critical concentration less than $c[\eta] = 8$. Rather, if the physical uncrossability affects the concentration dependence of the relaxation time, its effect becomes gradually more important with increasing concentration.

Relaxation Spectrum. For an unentangled polymer, the correlation in the end-to-end vector

$$\frac{\langle \mathbf{R}(t)\cdot\mathbf{R}(0)\rangle}{\langle \mathbf{R}^2\rangle} = \frac{8}{\pi^2}\sum_{p=\text{odd}}\frac{1}{p^2}e^{-t/\tau_p}, \quad \tau_p = \tau_1/p^2 \tag{23}$$

based on the Rouse model where τ_1 can be calculated using the zero-shear viscosity as discussed earlier in the context of eq 13. The tube model for entangled polymers predicts the same functional form for the correlation in the end-to-end vector with a different $\tau_1 = L^2/D_{\text{tube}}$ where L is the contour length of the primitive chain and D_{tube} is the diffusion coefficient along the tube.[5] Therefore, on the basis of these models for polymer melts, we expect entanglements to affect only the location of the peak but not its shape. Imanishi et al.[17] find that melts of both entangled and unentangled polymers show essentially identical normalized loss curves; that is, the entanglements do not affect the relaxation spectrum as gauged from the shape of the dielectric loss peak. Although this similarity in peak shape for entangled and unentangled polymers is consistent with the Rouse and tube models discussed above, the empirically observed spectrum is *broader* than that predicted by these models as shown in Figure 9. (As discussed earlier, the Rouse and Zimm spectra are indistinguishable over the range of dielectric loss considered here.) It has been shown that, for polyisoprene melts, much of the deviation of ϵ'' from the Rouse–tube prediction for $\omega\tau_1 < 10$ could be attributed to the polydispersity of the sample.[37] Based on measured (GPC) molecular weight distributions, it can be shown that, for the relatively monodisperse samples used in the present study, the low concentration data of Figure 9 are consistent with the polydispersity-corrected Rouse spectrum. However, for dilute (unentangled) solutions, polydispersity effects would have roughly the same effect on the shape of ϵ'' at all concentrations and could not cause the large change in loss peak breadth with increasing concentration. A direct comparison of our data with that for PI melts reported by Imanishi et al.[17] in Figure 9 shows that the deviations from the Rouse–tube model spectrum observed in PI melts are in fact *systematic* deviations that arise with increasing overlap between polymer coils. In other words, the Rouse–Zimm spectrum only provides an adequate description of the dynamics at low concentrations, namely, $c[\eta] \leq 1$, and the spectrum gradually broadens with increasing overlap between polymer molecules, apparently reaching the melt limit at $c[\eta] \approx 8$.[38]

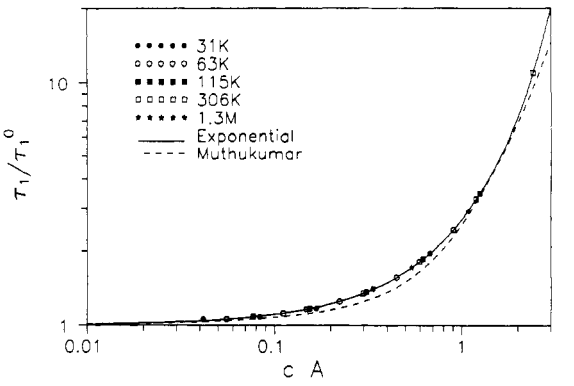

Figure 10. Reduced terminal relaxation time as a function of dimensionless concentration cA, where A is determined from the data of Figure 4. The theory of Muthukumar (dashed line) based on measured A values provides a reasonable prediction of the concentration dependence but does not fit the data as well as the simple exponential (solid line).

It is important to note that the relaxation spectrum for an unentangled polymer must also exhibit the same trends, namely, follow Rouse–Zimm dynamics at infinite dilution and gradually broaden with increasing concentration toward the melt spectrum (which does not depend on entanglements). This comparison also suggests that the observed concentration dependence of the relaxation spectrum is not related to entanglements. Therefore, on the basis of this argument, the observed broadening of the spectrum with increasing concentration from being Rouse–Zimm-like at low concentrations to meltlike at high concentrations is apparently *not* due to entanglement effects.

Screening of Excluded-Volume and Hydrodynamic Interactions. As discussed earlier, the Zimm model with dominant intramolecular hydrodynamic interactions provides an adequate description of polymer dynamics in the limit of infinite dilution. Both the excluded-volume and hydrodynamic interactions are expected to be progressively screened with increasing polymer concentration and this screening must affect the relaxation dynamics. The effects of these types of interactions on the dynamics of polymers are described in a theory by Muthukumar.[39] This theory predicts how the relaxation time of the pth mode τ_p changes with concentration starting from its Zimm value at τ_p^0 at infinite dilution. The result can be expressed as

$$\tau_p = \tau_p^0[1 + (Acp^{-\kappa}) - 2^{1/2}(Acp^{-\kappa})^{3/2} + 2(Acp^{-\kappa})^2 - ...] \tag{24}$$

where A is a positive constant obtained by the initial slope of a semilogarithmic plot of τ_1 as a function of c and κ is a positive exponent with a value 0.5 in Θ solvents and 0.65–0.80 in good solvents.

Longest Relaxation Time. Figure 10 shows a plot of the longest relaxation time τ_1 as a function of cA, where A is evaluated from the measured concentration dependence for each molecular weight (shown in Figure 4) as suggested by the Muthukumar theory. This figure clearly shows that the data for all molecular weights collapse onto a master curve. A comparison of Figures 8 and 10 shows that the collapse is noticeably better when the concen-

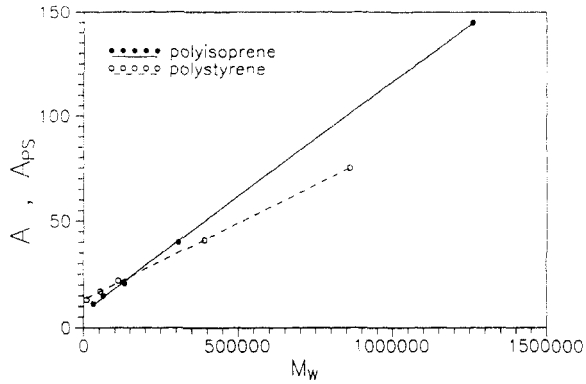

Figure 11. Molecular weight dependence of the concentration scaling parameter A. The polystyrene data were obtained by Martel et al.[9] using oscillatory flow birefringence measurements in Aroclor 1248.

tration is scaled by A rather then $[\eta]$. It must be noted that, with no adjustable parameters (A is fit from the low concentration data), the Muthukumar theory fits the longest relaxation time data reasonably well. However, a simple exponential dependence of the form

$$(\tau_1/\tau_1^0) = e^{cA} \tag{25}$$

fits the data even better, although it is, to our knowledge, strictly empirical and not predicted by any theory.

This successful collapse of the data to a master curve of the form described by eq 25, clearly hinges on the fact that the longest relaxation time for each molecular weight shows an exponential dependence over the entire concentration range as seen in Figure 4. A similar exponential dependence has been observed by Lodge, Schrag, and co-workers[9,40] using oscillatory flow birefringence measurements of polystyrene solutions in Aroclor over concentration ranges that were comparable to those of this study. The successful collapse of the longest relaxation time data in Figure 10 suggests that $1/A$ is the characteristic concentration appropriate for scaling the dynamics of polymer solutions. The values of A obtained from the slopes of the concentration dependence of the longest relaxation time, and used to obtain the master curve in Figure 10, are plotted as a function of M_w in Figure 11. The data are described well by a simple linear relation

$$A = \frac{1}{c_d}\left(1 + \frac{M_w}{M_d}\right) = \frac{1}{0.13}\left(1 + \frac{M_w}{70984}\right) \text{cm}^3/\text{g} \tag{26}$$

where c_d and M_d are the "characteristic" concentration and molecular weight suggested by such a linear fit. Although Martel et al.[9] do not fit their data using this functional form, we find that their data can also be fit by a similar expression

$$A_{PS} = \frac{1}{0.765}\left(1 + \frac{M_w}{181347}\right) \text{cm}^3/\text{g} \tag{27}$$

as shown in Figure 11. (We have added a subscript PS to differentiate between our data and that of Martel and co-workers.) The fact that the A for both PI and PS exhibits an intercept ($=1/c_d$) is suprising and suggests that the observed behavior might be related to a crossover despite the reasonably good linear fit obtained over a wide molecular weight range. Currently we do not offer any interpretation of the characteristic concentrations and molecular weights suggested by these fits although we speculate that these might be related to the critical concentration and molecular weight for entanglement usually measured viscoelastically.

Relaxation Spectrum. As discussed in the previous section, the Muthukumar theory provides a reasonable fit to the scaled longest relaxation time data in Figure 10 although the fit is better with a simple exponential. Besides the longest relaxation time, this theory also predicts the concentration dependence of the spectrum as expressed in eq 24. Muthukumar argues that the screening of hydrodynamic interactions resulting in a crossover from Zimm to Rouse dynamics must occur at fairly low concentrations. Although based on the current data we cannot track this crossover, the data in Figure 9 suggest that is probably occurs at fairly low values of $c[\eta]$, namely, $c[\eta] \leq 1$, indicating that very little overlap between molecules is required for the screening of hydrodynamic interactions.

As shown in Figure 9, our measurements show that the spectrum continues to broaden with concentration beyond the Rouse–Zimm limit and seems to become nearly identical to the melt spectrum at $c[\eta] \approx 8$. This behavior is considerably more profound than the intermolecular hydrodynamic interaction effect quantified by Muthukumar, which causes the spectrum to shift from the Zimm prediction at low concentration to Rouse behavior at finite concentrations $cA \sim 1$. Lodge et al.[9,40] also compare their data with the predictions of the Muthukumar theory. They report that, at low concentrations ($c[\eta] < 1$), the agreement is reasonable over most of the frequency range. However, akin to our findings, the data at higher concentrations and around the longest relaxation time do not seem to fit well by the Muthukumar theory. Our dielectric data, which emphasize the low-frequency part of the spectrum, underline this discrepancy.

The loss peaks plotted in Figure 9 suggest that the spectrum broadening is simply a function of the degree of overlap between molecules as gauged by $c[\eta]$. Unfortunately, the values of A and $[\eta]$ for the polymers for which the data are shown in Figure 9 are fortuitously such that the data at different molecular weights for which values of $c[\eta]$ coincide also have comparable values of cA. Therefore, on the basis of the current data, we cannot differentiate between a universal dependence based on a thermodynamic measure of overlap $c[\eta]$ or the dynamic measure of overlap cA. However, our data presented here combined with that of Imanishi and co-workers[17] for PI melts suggest that the broadening of the spectrum is related to the overlap between molecules but not to "entanglements" in the sense often implied in the polymer literature. To our knowledge, no theories have addressed this broadening of the spectrum with increasing overlap between polymer molecules and we hope that the apparent simplicity demonstrated by this study will stimulate some effort to address this issue.

Conclusions

We have probed the relaxation dynamics of polyisoprene in dilute and semidilute ($0.1 < c[\eta] < 8.15$) solutions in a marginal solvent using dielectric spectroscopy. The molecular weight of the narrow-distribution polyisoprene samples ranged from 3.1×10^4 to 3.3×10^6, allowing us to probe the dependences of molecular motions on both concentration and molecular weight. The solvent Isopar-G, a high-purity branched alkane, was a marginal solvent for polyisoprene with a MHS exponent of 0.7 and a Huggins coefficient of 0.42. We have found that both the terminal relaxation time and relaxation spectrum exhibit universal concentration dependences when concentration is scaled by the appropriate molecular weight dependent parameter.

The longest (terminal) relaxation time in the dilute limit was found to follow the form $\tau_1^0 = aM^{1.69}$. The exponent is consistent with both Rouse–Zimm and hard-sphere

models, which suggest that $\tau_1^0 \sim [\eta]M$. The coefficient a is intermediate between those predicted by Rouse and Zimm theories, suggesting that the molecules are partially draining. Terminal relaxation times were exponential in concentration, $\tau_1/\tau_1^0 = \exp(cA)$. The intrinsic viscosity $[\eta]$ was fairly successful as the concentration scaling parameter A, but best-fit A values had a somewhat different molecular weight dependence thant $[\eta]$. The concentration dependence of relaxation time showed no transition that would be indicative of entanglement effects, and the intermolecular hydrodynamic interaction theory of Muthukumar provided a fair prediction of the concentration dependence.

The relaxation spectrum, as it is reflected in the shape of the dielectric loss peak, appeared to be a universal function of $c[\eta]$ or cA. At low concentrations ($c[\eta] < 1$), the spectrum is consistent with that predicted by Rouse–Zimm theory, while for $c[\eta] > 1$ the loss peak is markedly broader than that allowed by Rouse–Zimm theory. When $c[\eta] \geq 8$, both coil dimensions and relaxation spectra approach values that are found in polyisoprene melts. The change in the spectrum with concentration goes far beyond that predicted by Muthukumar theory, which predicts a shift in spectrum from the Zimm limit to Rouse-like behavior as hydrodynamic interactions are screened (dimensionless concentration $cA \approx 1$). We show that the relaxation spectrum is a universal function of the degree of overlap between polymer coils. The results have important implications about the dynamics of main-chain relaxations and will be the subject of continuing study.

Acknowledgment. We thank S. Matsuoka, T. Lodge, K. Osaki, R. Larson, V. Raju, M. Muthukumar, E. Helfand, K. Amundson, X. Quan, D. Douglass, G. Johnson, S. Muller, and K. Winey for several fruitful discussions at various stages of this project over the last 2 years. We also acknowledge Professor T. Kotaka's group at Osaka University, whose work inspired this study.

References and Notes

(1) The angular brackets represent an ensemble average. Such an average will be implicit for all the properties discussed in this paper, and the brackets will only by used to stress this fact wherever necessary.
(2) Flory, P. J. *Principles of Polymer Chemistry*; Cornell University Press: Ithaca, NY, 1953.
(3) Ferry, J. D. *Viscoelastic Properties of Polymers*, 3rd ed.; John Wiley and Sons: New York, 1980.
(4) Bird, R. B.; Curtiss, C. F.; Armstrong, R. C.; Hassager, O. *Dynamics of Polymeric Liquids*, 2nd ed.; John Wiley and Sons: New York, 1987; Vol. 2.
(5) Doi, M.; Edwards, S. F. *The Theory of Polymer Dynamics*; Oxford University Press: New York, 1986.
(6) Rouse, P. E. *J. Chem. Phys.* **1953**, *21*, 1272.
(7) Tirrell, M. *Rubber Chem. Technol.* **1984**, *57*, 523.
(8) Johnson, R. M.; Schrag, J. L.; Ferry, J. D. *Polymer (Jpn.)* **1970**, *1*, 742. Massa, D. J.; Schrag, J. L.; Ferry, J. D. *Macromolecules* **1971**, *4*, 210. Osaki, K.; Mitsuda, Y.; Johnson, R. M.; Schrag, J. L.; Ferry, J. D. *Macromolecules* **1972**, *5*, 17. Lodge, T. P.; Miller, J. P.; Schrag, J. L. *J. Polym. Sci.* **1982**, *20*, 1409.
(9) Martel, C. J. T.; Lodge, T. P.; Dibbs, M. G.; Stokich, T. M.; Sammler, R. L.; Carriere, C. J.; Schrag, J. L. *Faraday Symp. Chem. Soc.* **1983**, *18*, 173.
(10) For a more detailed discussion of the different aspects probe by different techniques, see: Doi, M.; Edwards, S. F. Reference 5. Watanabe, H.; Tirrell, M. *Macromolecule* **1989**, *22*, 927. Watanabe, H.; Yamazaki, M.; Yoshida, H.; Kotaka, K. *Macromolecules* **1991**, *24*, 5365, 5372, 5573.
(11) Stockmayer, W. H. *Pure Appl. Chem.* **1967**, *15*, 539. Stockmayer, W. H.; Baur, M. E. *J. Am. Chem. Soc.* **1964**, *86*, 3485. Jones, A.; Brehm, G.; Stockmayer, W. *J. Polym. Sci., Polym. Symp.* **1974**, *46*, 149.
(12) Cole, R. H. *J. Chem. Phys.* **1965**, *42*, 637.
(13) Williams, G.; Watts, D. C. *Trans. Faraday Soc.* **1970**, *66*, 80.
(14) Takahashi, Y.; Isono, Y.; Noda, I.; Nagasawa, M. *Macromolecules* **1985**, *18*, 1002.
(15) Adachi, K.; Kotaka, T. *Macromolecules* **1984**, *17*, 120.
(16) Adachi, K.; Okazaki, H.; Kotaka, T. *Macromolecules* **1985**, *18*, 1687.
(17) Imanishi, Y.; Adachi, K.; Kotaka, T. *J. Chem. Phys.* **1988**, *89*, 7585. Adachi, K.; Kotaka, T. *Macromolecules* **1985**, *18*, 466.
(18) Yoshida, H.; Adachi, K.; Watanabe, H.; Kotaka, T. *Polym. J.* **1989**, *21*, 863. Adachi, K.; Imanishi, Y.; Kotaka, T. *J. Chem. Soc., Faraday Trans. 1* **1989**, *85*, 1065.
(19) Adachi, K.; Imanishi, Y.; Shinkado, T.; Kotaka, T. *Macromolecules* **1989**, *22*, 2391. Adachi, K.; Nakamoto, T.; Kotaka, T. *Macromolecules* **1989**, *22*, 3106–3111, 3111–3116. Adachi, K.; Nishi, I.; Itoh, S.; Kotaka, T. *Macromolecules* **1990**, *23*, 2550–2554, 2554–2559. Adachi, K.; Yoshida, H.; Fukui, F.; Kotaka, T. *Macromolecules* **1990**, *23*, 3138. Yoshida, H.; Watanabe, H.; Adachi, K.; Kotaka, T. *Macromolecules* **1991**, *24*, 2981.
(20) Boese, D.; Kremer, F. *Macromolecules* **1990**, *23*, 829. Boese, D.; Kremer, F.; Fetters, L. J. *Macromol. Chem., Rapid Commun.* **1988**, *9*, 367; *Macromolecules* **1990**, *23*, 1826.
(21) Graessley, W. W. *Adv. Polym. Sci.* **1974**, *16*, 1.
(22) Brandrup, J.; Immergut, E. H., Eds. *Polymer Handbook*, 3rd ed.; John Wiley and Sons: New York, 1989.
(23) Tsunashima, Y.; Hirata, M.; Nemoto, N.; Kurata, M. *Macromolecules* **1988**, *21*, 1107.
(24) Noda, I.; Yamada, Y.; Nagasawa, M. *J. Phys. chem.* **1968**, *72*, 2890.
(25) Larson, R. G. *Constitutive Equations for Polymer Melts and Solutions*; Butterworths: Boston, 1988.
(26) The Deborah number De is a dimensionless number defined as a ratio of the molecular relaxation time to the time scale of the experiment. Thus, when $De \ll 1$, the molecule can relax on the experimental time scale, whereas when $De \gg 1$ the molecule cannot do so. In steady shear, the experimental time scale is $\dot{\gamma}^{-1}$.
(27) Tanford, C. *Physical Chemistry of Macromolecules*; John Wiley and Sons: New York, 1961.
(28) Zimm, R. H. *J. Chem. Phys.* **1956**, *24*, 269.
(29) Throughout this paper we use the term "relaxation" in a generic sense referring to the response of the system when it is forced away from its equilibrium state. Strictly, the $g(\tau)$ measured dielectrically should be referred to as the "retardation" spectrum in common rheology parlance, by virtue of the fact that the contribution of the high-frequency modes *decreases* with increasing mode number.[3] (For the relaxation spectrum, all modes have *equal* contributions.) We are grateful to Shiro Matsuoka for drawing our attention to this fact.
(30) Frisch, H. L.; Simha, R. *Rheology*; Eirich, F. R., Ed.; Academic Press: New York, 1956.
(31) Noda, I.; Higo, Y.; Ueno, T.; Fujimoto, T. *Macromolecules* **1984**, *17*, 1055.
(32) Daoud, M.; Cotton, J. P.; Farnoux, B.; Jannink, G.; Sarma, G.; Benoit, H.; Duplessix, R.; Picot, C.; de Gennes, P.-G. *Macromolecules* **1975**, *8*, 804.
(33) Utracki, L.; Simha, R. *J. Polym. Sci., Part A* **1963**, *1*, 1089. Simha, R.; Utracki, L. *J. Polym. Sci., Polym. Phys. Ed.* **1967**, *5*, 853.
(34) Takahashi, Y.; et al. References 14 and references therein.
(35) Osaki, K.; Nishizawa, K.; Kurata, M. *Macromolecules* **1982**, *15*, 1068.
(36) J. Gotro and W. W. Graessley (*Macromolecules* **1984**, *17*, 2767) report the critical molecular weight for entanglements $M_e \approx 10\,000$ for PI melts. We use $M_e = M_c/2$, as is the case for several polymers.[3]
(37) Watanabe, H.; Yamazaki, M.; Yoshida, H.; Kotaka, T. *Macromolecules* **1991**, *24*, 5372.
(38) The dielectric loss at high frequencies is higher in melts than for the solutions as shown in Figure 9 because of the proximity of the segmental mode relaxations in melts.[17] If this contribution is subtracted from the melt peak, the agreement between the high concentration and melt data is better. However, this subtraction requires the use of a model, and for the sake of simplicity we do not correct for this segmental mode contribution in the PI melt data.
(39) Muthukumar, M. *Macromolecules* **1984**, *17*, 971. Muthukumar, M.; Freed, K. F. *Macromolecules* **1978**, *11*, 843.
(40) Lodge, T. P.; Schrag, J. L. *Macromolecules* **1982**, *15*, 1376. Amelar, S.; Eastman, C. E.; Morris, R. L.; Smeltzly, M. A.; Lodge, T. P. *Macromolecules* **1991**, *24*, 3505.

Registry No. PI (homopolymer), 9003-31-0.